What are the data needed to constrain and refine models ?

Frédéric Nowacki[1]

Confrontation and Convergence in Nuclear Theory
ECT* Trento, 27-31 July 2009

powered by LaTeX

[1] Strasbourg-Madrid-GSI Shell-Model collaboration

What are the data needed to constrain and refine models ?

THE DRAMA:

What are the data needed to constrain and refine models ?

THE DRAMA:

- Theorists here in the room :

  "None ! We don't need any !"

What are the data needed to constrain and refine models ?

THE DRAMA:

- Theorists here in the room :

  "None ! We don't need any !"

- Alexandra, Bill, Dieter, John, Magda, Olivier, Robert:

  "All of them ! Let's measure all of them !"

What are the data needed to constrain and refine models ?

THE DRAMA:

- Theorists here in the room :

  "None ! We don't need any !"

- Alexandra, Bill, Dieter, John, Magda, Olivier, Robert:

  "All of them ! Let's measure all of them !"

Fortunately, life has made us more reasonable ...

Shell structure and correlations

- at stability
  - double magicity + superdeformed states: ^{16}O, ^{40}Ca, ^{56}Ni
- far from stability
  - Vanishing of shell closure: ^{11}Li, ^{32}Mg, ^{42}Si, ^{68}Ni, ^{80}Zr ...
  - New gaps: ^{24}O, ^{54}Ca ...

Interplay between
- Monopole field (spherical mean field)
- Multipole correlations (pairing, Q.Q, ...)

“Pairing plus Quadrupole propose, Monopole disposes”

A. Zuker, Coherent and Random Hamiltonians, CRN Preprint 1994

For the Monopole field itself,

interplay between
- single particle field
- two-body interaction (T=1, T=0)

Evolution of nuclear shells due to Tensor force

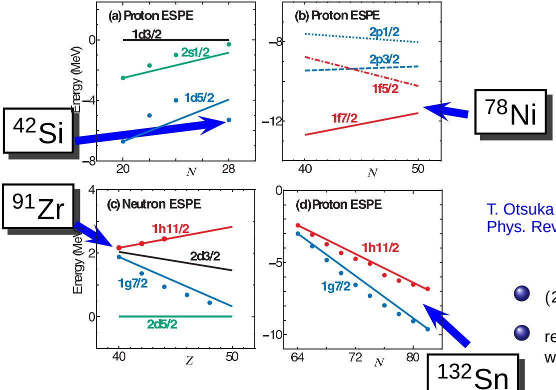

FIG. 4 (color). Proton (neutron) ESPE as a function of N (Z). Lines in (a)–(c) show the change of ESPE's calculated from the $\pi + \rho$ tensor force. Points represent the corresponding experimental data. (a) Proton ESPE's in Ca isotopes relative to $1d_{3/2}$. Points are from [13]. (b) Proton ESPE's in Ni isotopes; calculations only. See [19] for related experimental data. (c) Neutron ESPE's in $N = 51$ isotones relative to $2d_{5/2}$; points are from [21]. (d) Proton ESPE's in Sb isotopes; points are from [18]. Lines include a common shift of ESPE as well as the tensor effect (see the text).

T. Otsuka et al.,
Phys. Rev. Lett. **95**, 232502-1 (2005)

- $(2j_> + 1)V^T_{j_>,j'} + (2j_< + 1)V^T_{j_<,j'} = 0,$
- reduction of spin-orbit partners splitting while filling j' shell

Effective single particle energies and neutron gap evolution

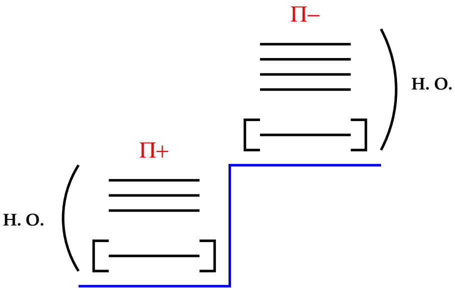

- unstable ^{42}Si, ^{78}Ni and ^{132}Sn have a BB, stable ^{208}Pb
- at first order, they result of the filling of a $j_> = l + \frac{1}{2}$ proton orbital and a $j'_> = l + 1 + \frac{1}{2}$ neutron orbital of opposite parities
- $j_> = d_{\frac{5}{2}}$ $j'_> = f_{\frac{7}{2}}$ for ^{42}Si,
  $j_> = f_{\frac{7}{2}}$ $j'_> = g_{\frac{9}{2}}$ for ^{78}Ni,
  $j_> = g_{\frac{9}{2}}$ $j'_> = h_{\frac{11}{2}}$ for ^{132}Sn,
- one expects strong variation of shell structure away from this picture

Neutron rich nuclei: N=20

	J^π	exp	SDPF-U		J^π	exp	SDPF-U
^{35}Si	$\frac{7}{2}^-$	0.0	0.0	^{37}S	$\frac{7}{2}^-$	0.0	0.0
	$\frac{3}{2}^-$	0.91	0.93		$\frac{3}{2}^-$	0.65	0.62
	$\frac{1}{2}^-$	(2.0)	2.14		$\frac{5}{2}^-$	2.51	2.44
	$\frac{5}{2}^-$	—	4.16		$\frac{1}{2}^-$	2.64	2.61
^{39}Ar	$\frac{7}{2}^-$	0.0	0.0	^{41}Ca	$\frac{7}{2}^-$	0.0	0.0
	$\frac{3}{2}^-$	1.27	1.54		$\frac{3}{2}^-$	2.50	2.50
	$\frac{5}{2}^-$	2.09	2.13		$\frac{1}{2}^-$	4.16	4.20
	$\frac{1}{2}^-$	—	3.08		$\frac{5}{2}^-$	6.98	6.99
^{47}K	$\frac{1}{2}^+$	0.0	0.0	^{49}K	$\frac{3}{2}^+$	0.0	0.0
	$\frac{3}{2}^+$	0.36	0.32		$\frac{1}{2}^+$	0.20	0.08
	$\frac{5}{2}^+$	3.32	3.06		$\frac{5}{2}^+$	0.77	0.70
^{49}Ca	$\frac{3}{2}^-$	0.0	0.0	^{47}Ar	$\frac{3}{2}^-$	0.0	0.0
	$\frac{1}{2}^-$	2.02	1.96		$\frac{5}{2}^-$	—	1.27
	$\frac{7}{2}^-$	3.35	3.14		$\frac{1}{2}^-$	1.13	1.12
	$\frac{5}{2}^-$	3.99	4.03		$\frac{7}{2}^-$	1.74	1.57

Neutron rich nuclei: N=20 New

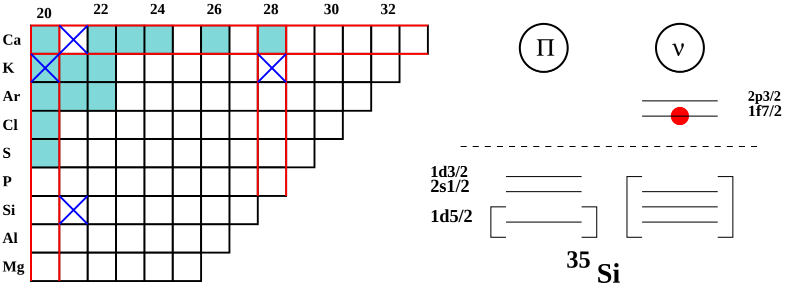

Neutron rich nuclei: N=20 New

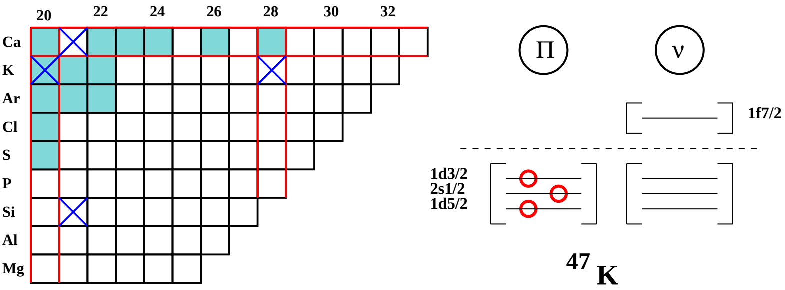

Neutron rich nuclei: N=20

	J^π	exp	SDPF-U		J^π	exp	SDPF-U
^{35}Si	$\frac{7}{2}^-$	0.0	0.0	^{37}S	$\frac{7}{2}^-$	0.0	0.0
	$\frac{3}{2}^-$	0.91	0.93		$\frac{3}{2}^-$	0.65	0.62
	$\frac{1}{2}^-$	(2.0)	2.14		$\frac{3}{2}^-$	2.51	2.44
	$\frac{5}{2}^-$	—	4.16		$\frac{5}{2}^-$	2.64	2.61
^{39}Ar	$\frac{7}{2}^-$	0.0	0.0	^{41}Ca	$\frac{7}{2}^-$	0.0	0.0
	$\frac{3}{2}^-$	1.27	1.54		$\frac{3}{2}^-$	2.50	2.50
	$\frac{5}{2}^-$	2.09	2.13		$\frac{1}{2}^-$	4.16	4.20
	$\frac{1}{2}^-$	—	3.08		$\frac{5}{2}^-$	6.98	6.99
^{47}K	$\frac{1}{2}^+$	0.0	0.0	^{49}K	$\frac{3}{2}^+$	0.0	0.0
	$\frac{3}{2}^+$	0.36	0.32		$\frac{1}{2}^+$	0.20	0.08
	$\frac{5}{2}^+$	3.32	3.06		$\frac{5}{2}^+$	0.77	0.70
^{49}Ca	$\frac{3}{2}^-$	0.0	0.0	^{47}Ar	$\frac{3}{2}^-$	0.0	0.0
	$\frac{1}{2}^-$	2.02	1.96		$\frac{5}{2}^-$	—	1.27
	$\frac{7}{2}^-$	3.35	3.14		$\frac{1}{2}^-$	1.13	1.12
	$\frac{5}{2}^-$	3.99	4.03		$\frac{7}{2}^-$	1.74	1.57

what have we learnt?

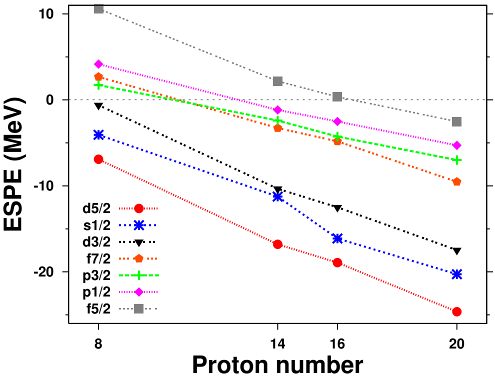

- reduction of $f_{\frac{7}{2}} - d_{\frac{3}{2}}$ N=20 gap
  emptying the $d_{\frac{3}{2}}$ proton orbital
- reduction of $p_{\frac{3}{2}} - p_{\frac{1}{2}}$ so splitting
  with filling of $s_{\frac{1}{2}}$ proton orbital
- reduction of $f_{\frac{7}{2}} - p_{\frac{3}{2}}$ N=28 gap
  with filling of $d_{\frac{3}{2}}$ neutron orbital

→ Development of "Island of deformation" around A=32

what have we learnt?

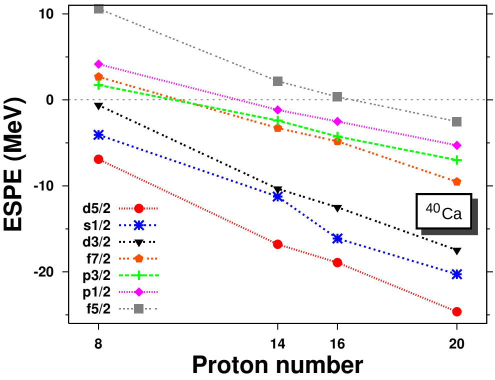

- reduction of $f_{\frac{7}{2}} - d_{\frac{3}{2}}$ N=20 gap
  emptying the $d_{\frac{3}{2}}$ proton orbital
- reduction of $p_{\frac{3}{2}} - p_{\frac{1}{2}}$ so splitting
  with filling of $s_{\frac{1}{2}}$ proton orbital
- reduction of $f_{\frac{7}{2}} - p_{\frac{3}{2}}$ N=28 gap
  with filling of $d_{\frac{3}{2}}$ neutron orbital

→ Development of "Island of deformation" around A=32

what have we learnt?

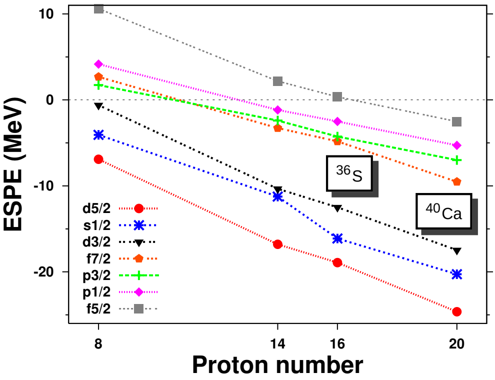

- reduction of $f_{\frac{7}{2}} - d_{\frac{3}{2}}$ N=20 gap
  emptying the $d_{\frac{3}{2}}$ proton orbital
- reduction of $p_{\frac{3}{2}} - p_{\frac{1}{2}}$ so splitting
  with filling of $s_{\frac{1}{2}}$ proton orbital
- reduction of $f_{\frac{7}{2}} - p_{\frac{3}{2}}$ N=28 gap
  with filling of $d_{\frac{3}{2}}$ neutron orbital

→ Development of "Island of deformation" around A=32

what have we learnt?

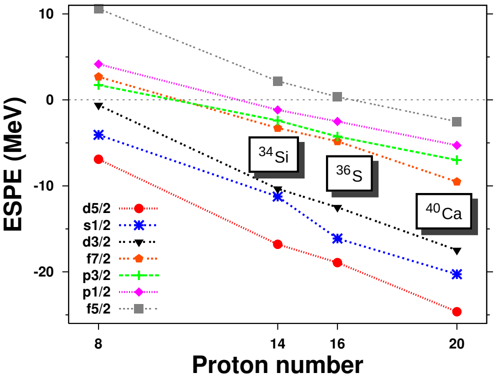

- reduction of $f_{\frac{7}{2}} - d_{\frac{3}{2}}$ N=20 gap
  emptying the $d_{\frac{3}{2}}$ proton orbital
- reduction of $p_{\frac{3}{2}} - p_{\frac{1}{2}}$ so splitting
  with filling of $s_{\frac{1}{2}}$ proton orbital
- reduction of $f_{\frac{7}{2}} - p_{\frac{3}{2}}$ N=28 gap
  with filling of $d_{\frac{3}{2}}$ neutron orbital

→ Development of "Island of deformation" around A=32

what have we learnt?

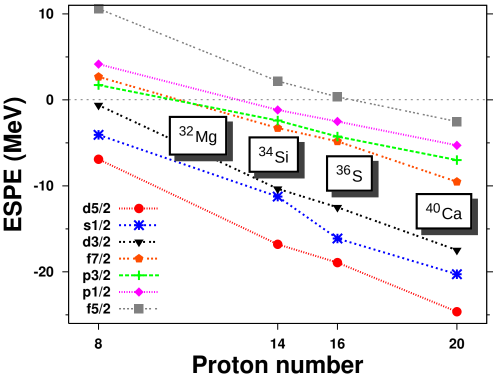

- reduction of $f_{\frac{7}{2}} - d_{\frac{3}{2}}$ N=20 gap
  emptying the $d_{\frac{3}{2}}$ proton orbital
- reduction of $p_{\frac{3}{2}} - p_{\frac{1}{2}}$ so splitting
  with filling of $s_{\frac{1}{2}}$ proton orbital
- reduction of $f_{\frac{7}{2}} - p_{\frac{3}{2}}$ N=28 gap
  with filling of $d_{\frac{3}{2}}$ neutron orbital

→ Development of "Island of deformation" around A=32

what have we learnt?

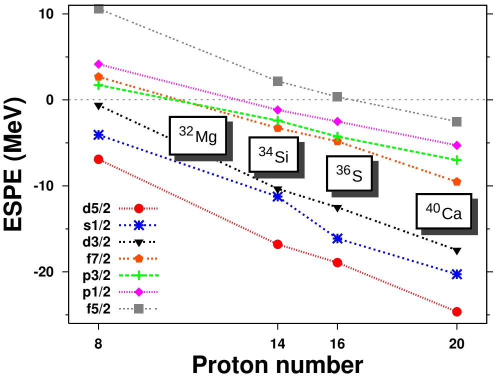

- reduction of $f_{\frac{7}{2}} - d_{\frac{3}{2}}$ N=20 gap
  emptying the $d_{\frac{3}{2}}$ proton orbital
- reduction of $p_{\frac{3}{2}} - p_{\frac{1}{2}}$ so splitting
  with filling of $s_{\frac{1}{2}}$ proton orbital
- reduction of $f_{\frac{7}{2}} - p_{\frac{3}{2}}$ N=28 gap
  with filling of $d_{\frac{3}{2}}$ neutron orbital

→ Development of "Island of deformation" around A=32

Spin-Tensor analysis done by K. Sieja

Spin-Tensor decomposition

$f_{\frac{7}{2}}$-$d_{\frac{3}{2}}$ Gap evolution between ^{32}Mg and ^{34}Si

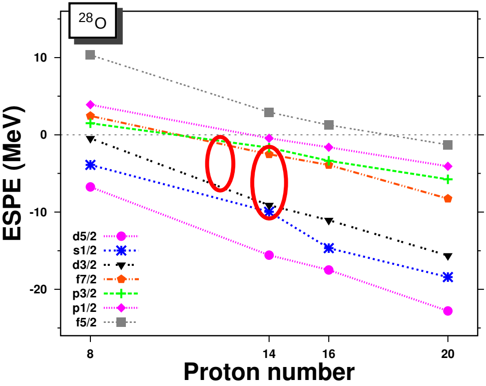

Δ	$f_{\frac{7}{2}}$-$d_{\frac{3}{2}}$ Gap
Tot	+1.17
central	+0.70
ALS	+0.12
LS	-0.067
tensor	+0.66

SDPF-U

powered by LaTeX

Spin-Tensor decomposition

$f_{\frac{7}{2}}$-$d_{\frac{3}{2}}$ Gap evolution between ^{32}Mg and ^{34}Si

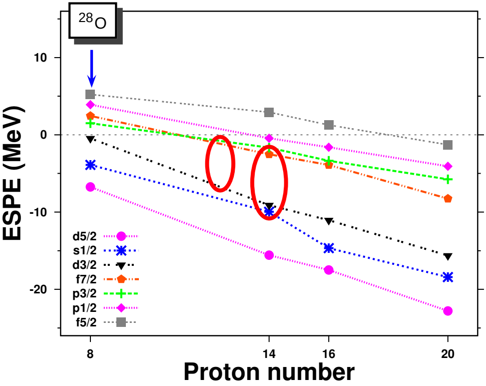

- SDPF-U

Δ	$f_{\frac{7}{2}}$-$d_{\frac{3}{2}}$ Gap
Tot	+1.17
central	+0.70
ALS	+0.12
LS	-0.067
tensor	+0.66

- SDPF-Umod

$$\Delta V^{T=1}_{d_{\frac{5}{2}} f_{\frac{5}{2}}} = -1.0 \text{ MeV}$$

$$\Delta V^{T=0}_{d_{\frac{5}{2}} f_{\frac{5}{2}}} = +3.0 \text{ MeV}$$

Spin-Tensor decomposition

$f_{\frac{7}{2}}$-$d_{\frac{3}{2}}$ Gap evolution between ^{32}Mg and ^{34}Si

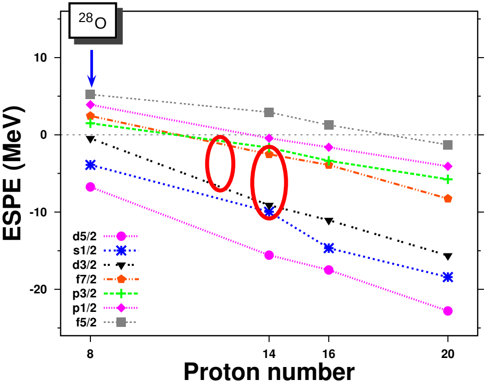

SDPF-U

Δ	$f_{\frac{7}{2}}$-$d_{\frac{3}{2}}$ Gap
Tot	+1.17
central	+0.70
ALS	+0.12
LS	-0.067
tensor	+0.66

SDPF-Umod

$$\Delta V^{T=1}_{d_{\frac{5}{2}} f_{\frac{5}{2}}} = -1.0 \text{ MeV}$$

$$\Delta V^{T=0}_{d_{\frac{5}{2}} f_{\frac{5}{2}}} = +3.0 \text{ MeV}$$

SDPF-Umod

Δ	$f_{\frac{7}{2}}$-$d_{\frac{3}{2}}$ Gap
Tot	+1.17
central	+1.09
ALS	-0.28
LS	-0.14
tensor	+0.51

what have we learnt?

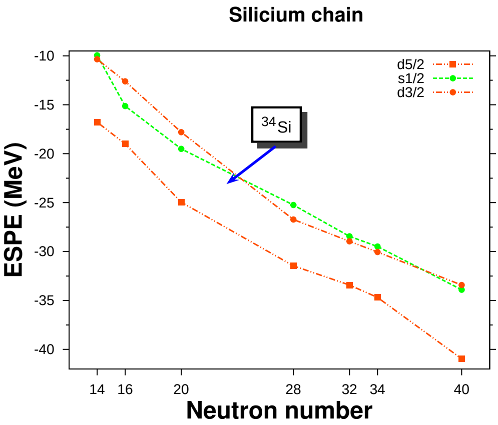

- reduction of $d_{\frac{5}{2}} - d_{\frac{3}{2}}$ Z=14 gap with filling of $f_{\frac{7}{2}}$ neutron orbital
- reduction of $p_{\frac{3}{2}} - p_{\frac{1}{2}}$ so splitting with filling of $s_{\frac{1}{2}}$ proton orbital
- reduction of $f_{\frac{7}{2}} - p_{\frac{3}{2}}$ N=28 gap with filling of $d_{\frac{3}{2}}$ neutron orbital

→ Tensor mechanism at play

what have we learnt?

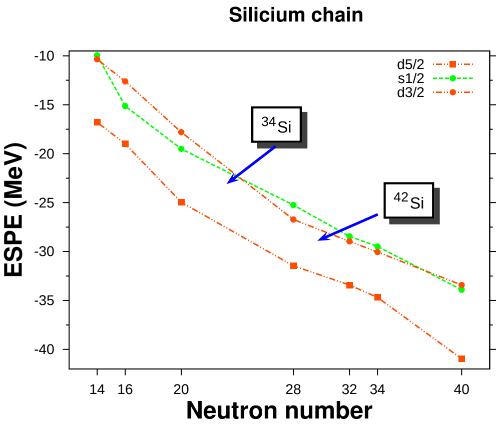

- reduction of $d_{\frac{5}{2}} - d_{\frac{3}{2}}$ Z=14 gap with filling of $f_{\frac{7}{2}}$ neutron orbital
- reduction of $p_{\frac{3}{2}} - p_{\frac{1}{2}}$ so splitting with filling of $s_{\frac{1}{2}}$ proton orbital
- reduction of $f_{\frac{7}{2}} - p_{\frac{3}{2}}$ N=28 gap with filling of $d_{\frac{3}{2}}$ neutron orbital

→ Tensor mechanism at play

what have we learnt?

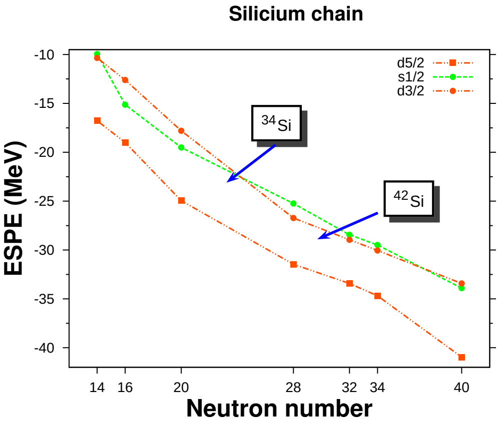

- reduction of $d_{\frac{5}{2}} - d_{\frac{3}{2}}$ Z=14 gap with filling of $f_{\frac{7}{2}}$ neutron orbital
- reduction of $p_{\frac{3}{2}} - p_{\frac{1}{2}}$ so splitting with filling of $s_{\frac{1}{2}}$ proton orbital
- reduction of $f_{\frac{7}{2}} - p_{\frac{3}{2}}$ N=28 gap with filling of $d_{\frac{3}{2}}$ neutron orbital

→ Tensor mechanism at play

Δ	$d_{\frac{5}{2}}$-$d_{\frac{3}{2}}$ Gap
Tot	-1.52
central	-0.23
ALS	+1.09
LS	+0.67
tensor	-3.05

SDPF-NR

what have we learnt?

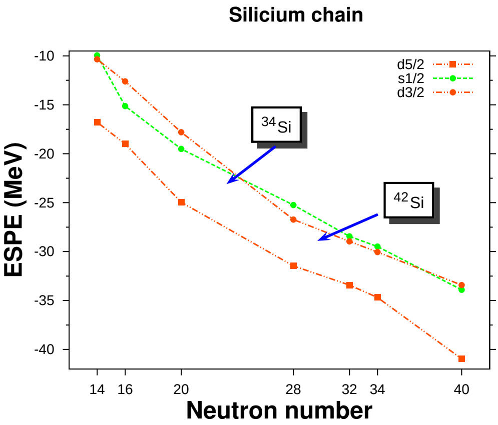

- reduction of $d_{\frac{5}{2}} - d_{\frac{3}{2}}$ Z=14 gap with filling of $f_{\frac{7}{2}}$ neutron orbital
- reduction of $p_{\frac{3}{2}} - p_{\frac{1}{2}}$ so splitting with filling of $s_{\frac{1}{2}}$ proton orbital
- reduction of $f_{\frac{7}{2}} - p_{\frac{3}{2}}$ N=28 gap with filling of $d_{\frac{3}{2}}$ neutron orbital

→ Tensor mechanism at play

Δ	$d_{\frac{5}{2}}$-$d_{\frac{3}{2}}$ Gap	
Tot	-2.49	SDPF-U
central	-0.23	
ALS	+0.60	
LS	+0.19	
tensor	-3.05	

Silicium and Magnesium chains

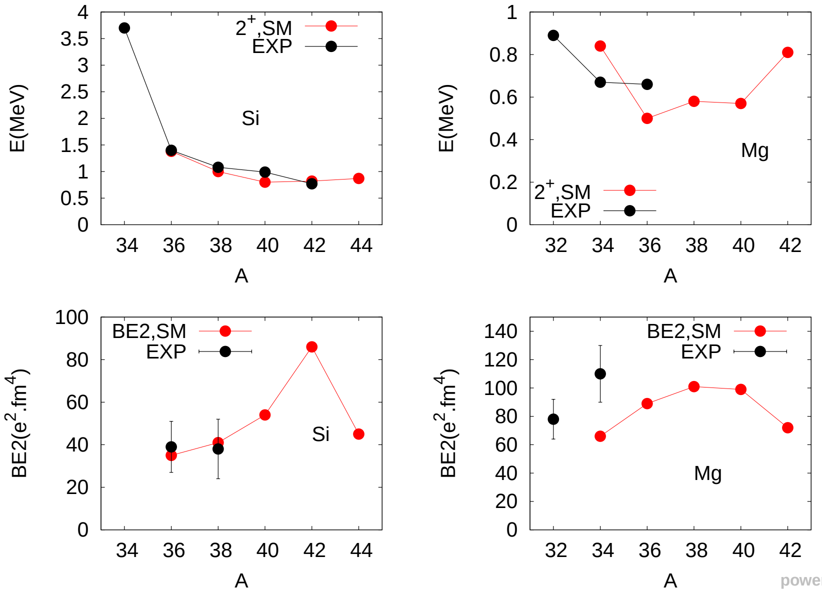

Silicium and Magnesium chains

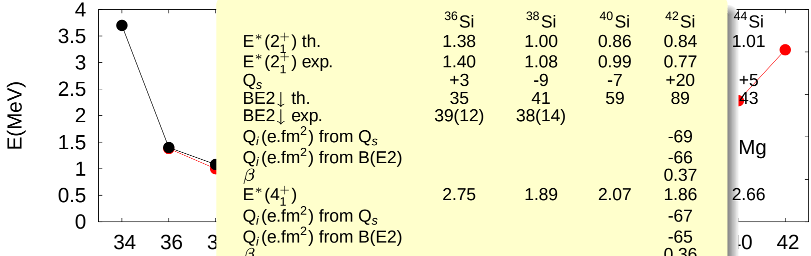

	^{36}Si	^{38}Si	^{40}Si	^{42}Si	^{44}Si
$E^*(2_1^+)$ th.	1.38	1.00	0.86	0.84	1.01
$E^*(2_1^+)$ exp.	1.40	1.08	0.99	0.77	
Q_s	+3	-9	-7	+20	+5
BE2↓ th.	35	41	59	89	43
BE2↓ exp.	39(12)	38(14)			
Q_i(e.fm^2) from Q_s				-69	
Q_i(e.fm^2) from B(E2)				-66	
β				0.37	
$E^*(4_1^+)$	2.75	1.89	2.07	1.86	2.66
Q_i(e.fm^2) from Q_s				-67	
Q_i(e.fm^2) from B(E2)				-65	
β				0.36	
S_{2n} th.	9.02	6.81	4.81	2.68	-0.08

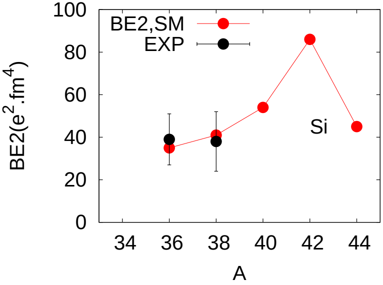

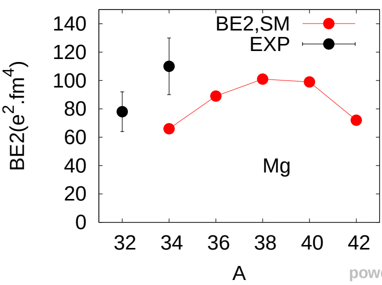

Silicium and Magnesium chains

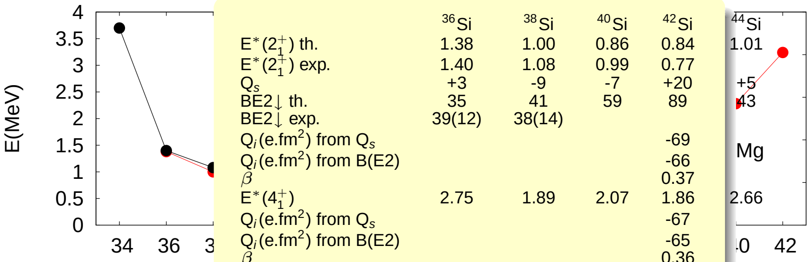

	^{36}Si	^{38}Si	^{40}Si	^{42}Si	^{44}Si
$E^*(2_1^+)$ th.	1.38	1.00	0.86	0.84	1.01
$E^*(2_1^+)$ exp.	1.40	1.08	0.99	0.77	
Q_s	+3	-9	-7	+20	+5
BE2↓ th.	35	41	59	89	43
BE2↓ exp.	39(12)	38(14)			
Q_i(e.fm^2) from Q_s				-69	
Q_i(e.fm^2) from B(E2)				-66	
β				0.37	
$E^*(4_1^+)$	2.75	1.89	2.07	1.86	2.66
Q_i(e.fm^2) from Q_s				-67	
Q_i(e.fm^2) from B(E2)				-65	
β				0.36	
S_{2n} th.	9.02	6.81	4.81	2.68	-0.08

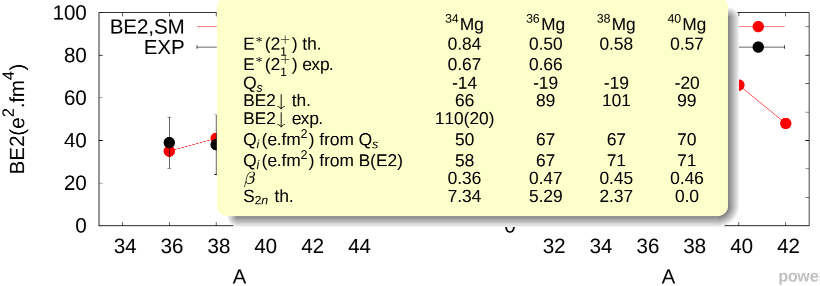

	^{34}Mg	^{36}Mg	^{38}Mg	^{40}Mg
$E^*(2_1^+)$ th.	0.84	0.50	0.58	0.57
$E^*(2_1^+)$ exp.	0.67	0.66		
Q_s	-14	-19	-19	-20
BE2↓ th.	66	89	101	99
BE2↓ exp.	110(20)			
Q_i(e.fm^2) from Q_s	50	67	67	70
Q_i(e.fm^2) from B(E2)	58	67	71	71
β	0.36	0.47	0.45	0.46
S_{2n} th.	7.34	5.29	2.37	0.0

powered by LaTeX

Spin-Tensor decomposition

$p_{\frac{1}{2}}$-$p_{\frac{3}{2}}$ Gap evolution between ^{34}Si and ^{36}S

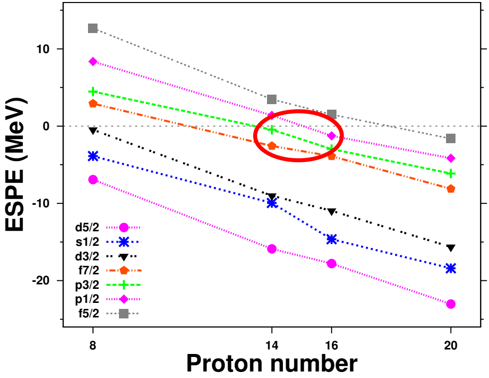

Δ	$p_{\frac{1}{2}}$-$p_{\frac{3}{2}}$ Gap	
Tot	-0.11	SDPF
central	+0.00	
ALS	-0.33	
LS	+0.22	
tensor	+0.00	

Spin-Tensor decomposition

$p_{\frac{1}{2}}$-$p_{\frac{3}{2}}$ Gap evolution between ^{34}Si and ^{36}S

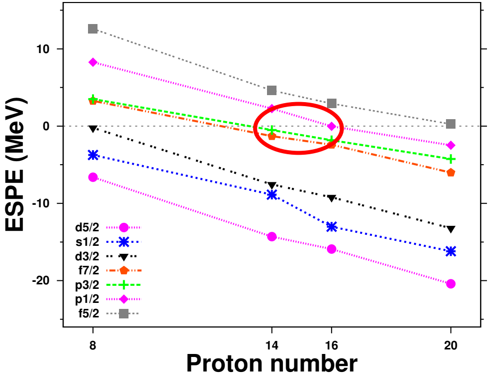

SDPF

Δ	$p_{\frac{1}{2}}$-$p_{\frac{3}{2}}$ Gap
Tot	-0.11
central	+0.00
ALS	-0.33
LS	+0.22
tensor	+0.00

SDPF-NR

Δ	$p_{\frac{1}{2}}$-$p_{\frac{3}{2}}$ Gap
Tot	-1.05
central	+0.00
ALS	-0.80
LS	-0.25
tensor	+0.00

Spin-Tensor decomposition

$p_{\frac{1}{2}}$-$p_{\frac{3}{2}}$ Gap evolution between ^{34}Si and ^{36}S

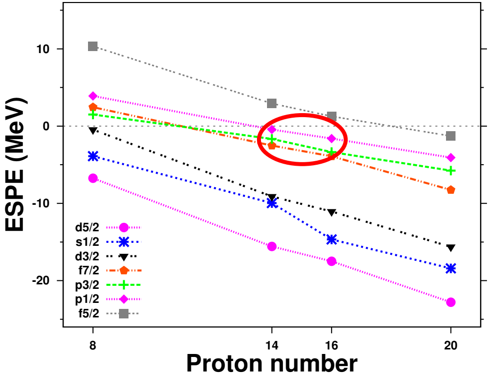

- SDPF

Δ	$p_{\frac{1}{2}}$-$p_{\frac{3}{2}}$ Gap
Tot	-0.11
central	+0.00
ALS	-0.33
LS	+0.22
tensor	+0.00

- SDPF-NR

Δ	$p_{\frac{1}{2}}$-$p_{\frac{3}{2}}$ Gap
Tot	-1.05
central	+0.00
ALS	-0.80
LS	-0.25
tensor	+0.00

- SDPF-U

Δ	$p_{\frac{1}{2}}$-$p_{\frac{3}{2}}$ Gap
Tot	+0.55
central	+0.00
ALS	-0.01
LS	+0.56
tensor	+0.00

what have we learnt?

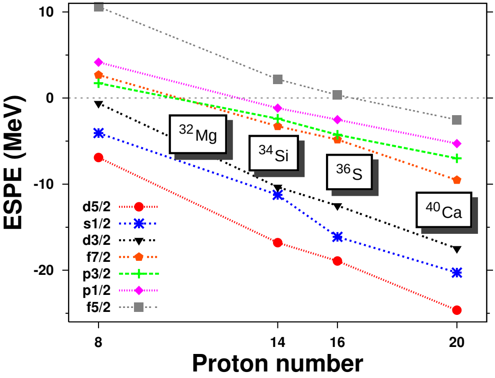

- increasing mismatch between 2^+ excitation energies for N=22 nuclei from ^{42}Ca to ^{36}Si
- similar effect as the one observed between ^{18}O to ^{16}C
- Is the NN interaction weaker far from stability ?
- Is it a pairing effect due to core polarization effects ?

Core polarization effects: N=22

Use of G matrix, Vlowk interactions + core polarization by Q box (2nd order)

from Morten Hjorth-Jensen

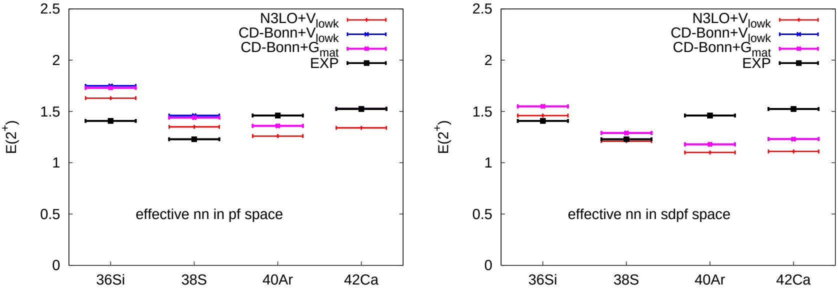

K. Sieja and F. N. in preparation

Core polarization effects: N=10

Use of G matrix, Vlowk interactions + core polarization by Q box (2nd order) from Morten Hjorth-Jensen

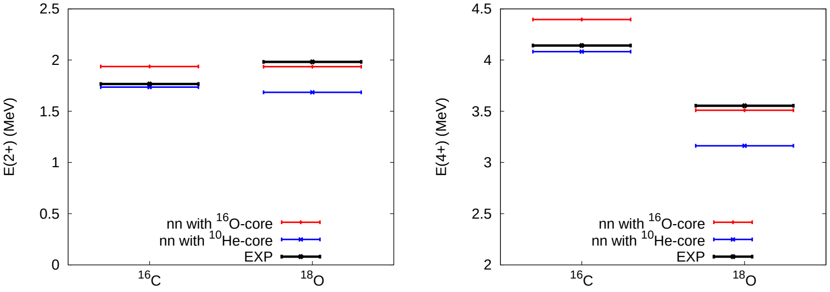

K. Sieja and F. N. in preparation

Clear transition between :

- No double closure for ^{20}C (N=14) and ^{42}Si (N=28)

→ Tensor mechanism at play

BUT

- Double closure for ^{132}Sn (N=82) and ^{208}Pb (N=126)

Transition region : ^{78}Ni (N=50)

AND
New Island of Inversion around ^{64}Cr

$50 \leq Z, N \leq 82$ region

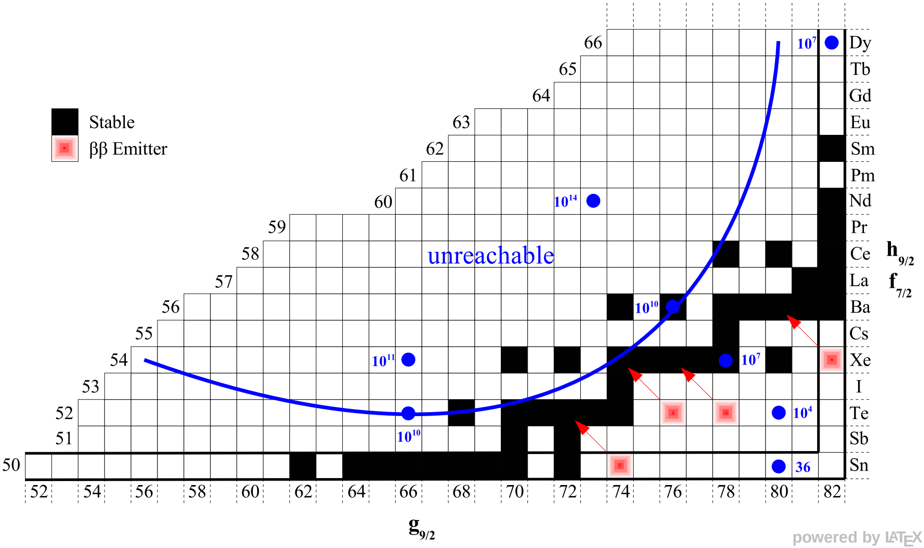

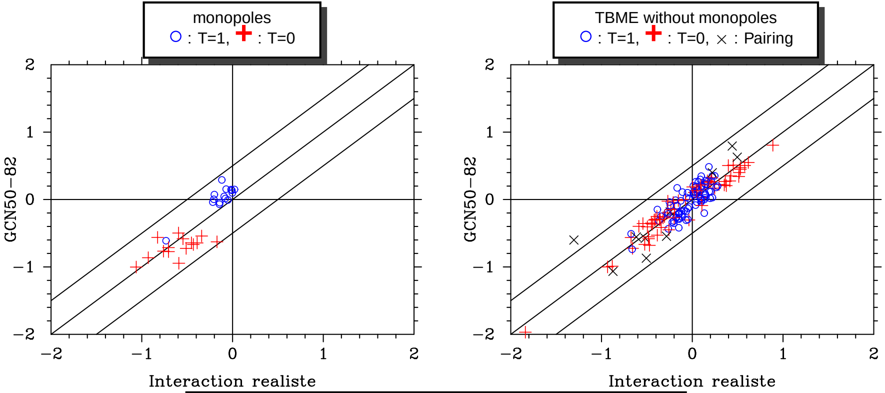

G Matrix† : $RMS = 1.200 MeV$
New interaction : $RMS = 0.110 MeV$

Fit on 385 exp. levels with 70 LC of TBME

† G matrix: M. Hjorth-Jensen, T.T.S. Kuo and E. Osnes, Realistic effective interactions for nuclear systems, Physics Reports 261 (1995) 125-270

Quadrupole excitations on CS nuclei

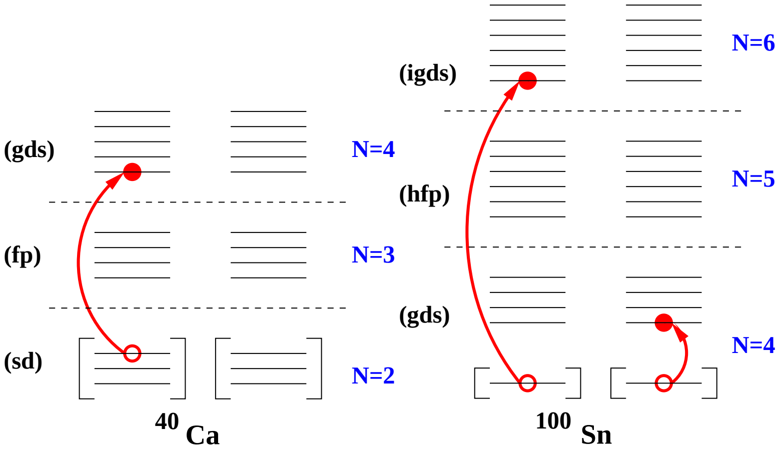

Core excitations in Tin isotopes

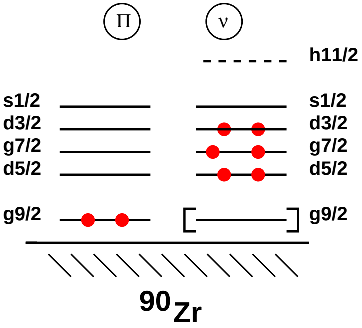

Advantages:

- avoids center of mass problem (non spurious)
- full space calculations feasible
- includes important correlations from $g_{\frac{9}{2}}$ and to $h_{\frac{11}{2}}$ shells

powered by LaTeX

Effective single particle energies and gap evolution

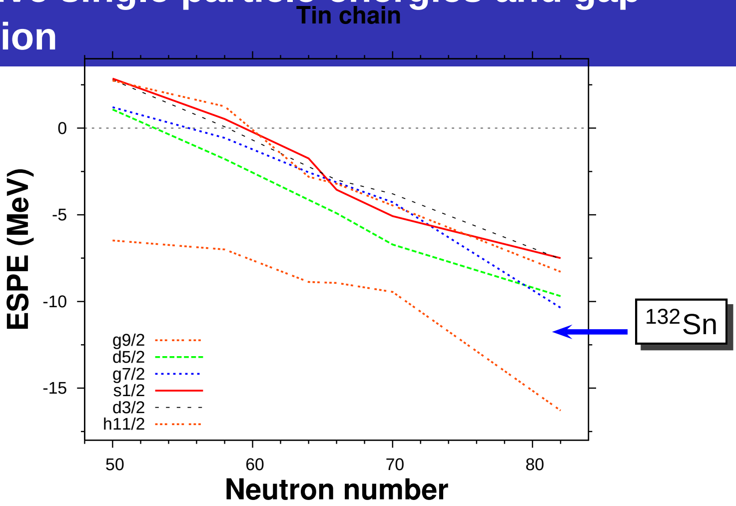

Proton gap (MeV)	exp.	ini.	gap a	gap b
130Sn	5.496	5.45	3.84	2.41
$h_{\frac{11}{2}}$ centroid(^{91}Zr)	2.17 (?)	6.5	5.0	3.5

powered by LaTeX

Effective single particle energies and gap evolution

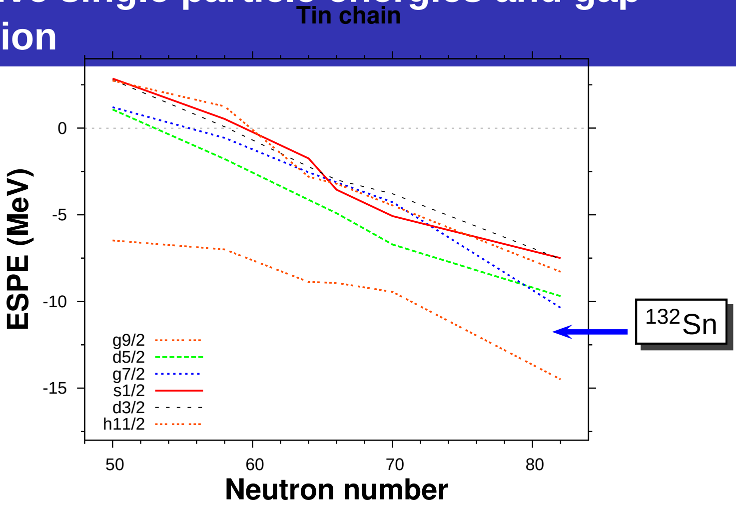

Proton gap (MeV)	exp.	ini.	gap a	gap b
130Sn	5.496	5.45	3.84	2.41
$h_{\frac{11}{2}}$ centroid(^{91}Zr)	2.17 (?)	6.5	5.0	3.5

Effective single particle energies and gap evolution

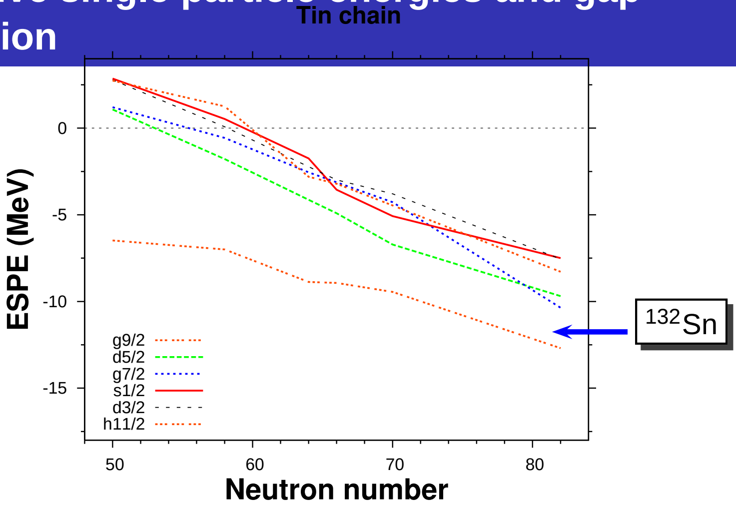

Proton gap (MeV)	exp.	ini.	gap a	gap b
130Sn	5.496	5.45	3.84	2.41
$h_{\frac{11}{2}}$ centroid(^{91}Zr)	2.17 (?)	6.5	5.0	3.5

B(E2)'s in Tin isotopes

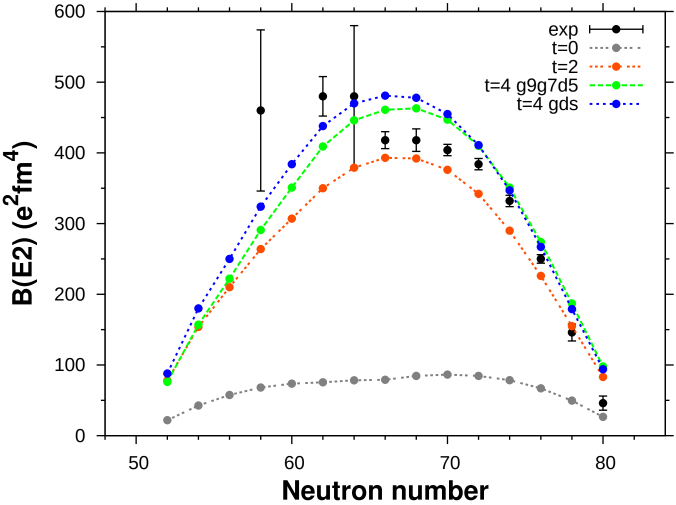

A. Banu et al.,

Phys. Rev. **C72**, 061305(R) (2005)

B(E2)'s in Tin isotopes

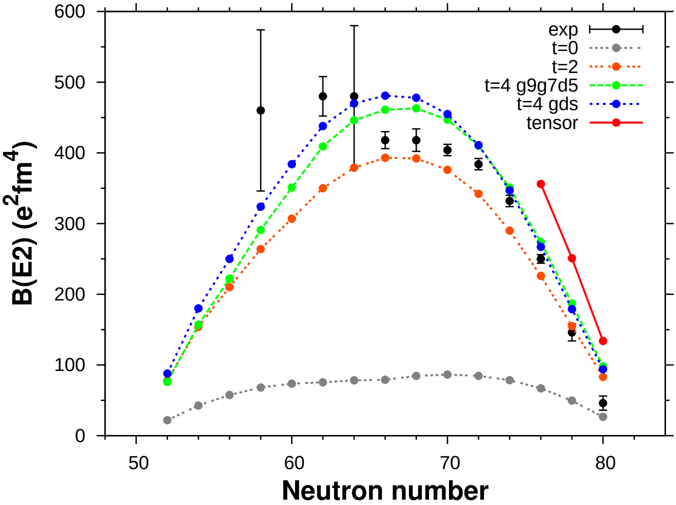

A. Banu et al.,

Phys. Rev. **C72**, 061305(R) (2005)

B(E2)'s in Tin isotopes

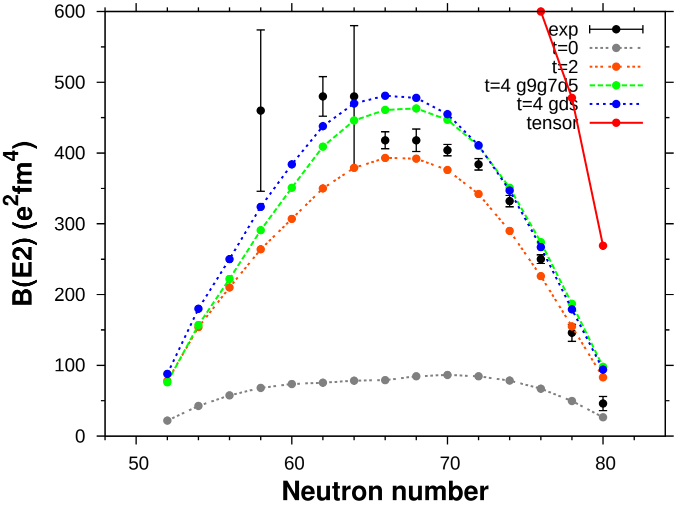

A. Banu et al.,

Phys. Rev. **C72**, 061305(R) (2005)

Core excitations in Tin isotopes

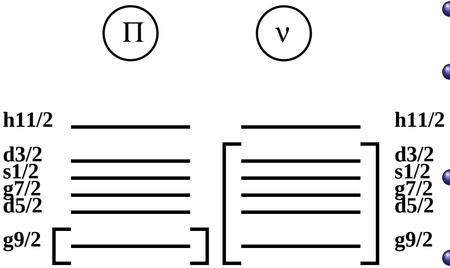

- 132 strongly bound
- low BE2 rates in Tin isotopes towards N=82
- strong proton-neutron attraction between $g_{\frac{7}{2}}$ and $h_{\frac{11}{2}}$ orbitals AND between $g_{\frac{9}{2}}$ and $h_{\frac{11}{2}}$ orbitals
- tensor force should be balanced by central and/or spin-orbit
- no visible tensor effect
- add $h_{\frac{9}{2}}$ for spin-tensor decomposition

Core excitations in Tin isotopes

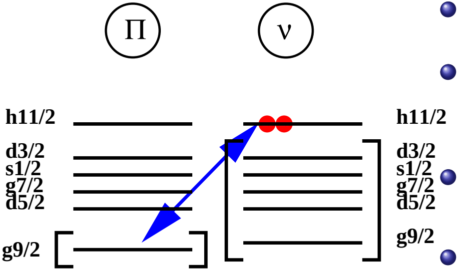

- 132 strongly bound
- low BE2 rates in Tin isotopes towards N=82
- strong proton-neutron attraction between $g_{\frac{7}{2}}$ and $h_{\frac{11}{2}}$ orbitals AND between $g_{\frac{9}{2}}$ and $h_{\frac{11}{2}}$ orbitals
- tensor force should be balanced by central and/or spin-orbit
- no visible tensor effect
- add $h_{\frac{9}{2}}$ for spin-tensor decomposition

Core excitations in Tin isotopes

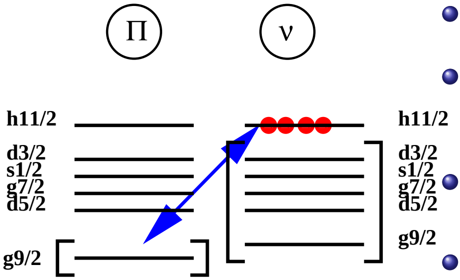

- 132 strongly bound
- low BE2 rates in Tin isotopes towards N=82
- strong proton-neutron attraction between $g_{\frac{7}{2}}$ and $h_{\frac{11}{2}}$ orbitals AND between $g_{\frac{9}{2}}$ and $h_{\frac{11}{2}}$ orbitals
- tensor force should be balanced by central and/or spin-orbit
- no visible tensor effect
- add $h_{\frac{9}{2}}$ for spin-tensor decomposition

Core excitations in Tin isotopes

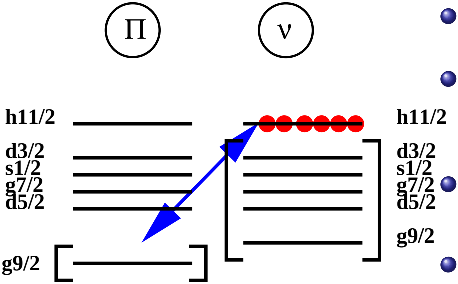

- ^{132} strongly bound
- low BE2 rates in Tin isotopes towards N=82
- strong proton-neutron attraction between $g_{\frac{7}{2}}$ and $h_{\frac{11}{2}}$ orbitals AND between $g_{\frac{9}{2}}$ and $h_{\frac{11}{2}}$ orbitals
- tensor force should be balanced by central and/or spin-orbit
- no visible tensor effect
- add $h_{\frac{9}{2}}$ for spin-tensor decomposition

Core excitations in Tin isotopes

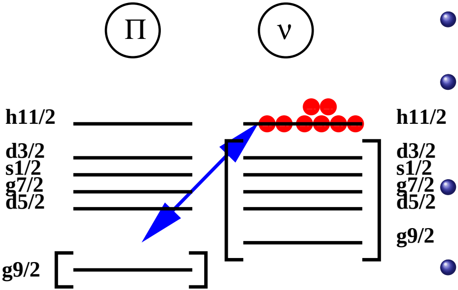

- ^{132} strongly bound
- low BE2 rates in Tin isotopes towards N=82
- strong proton-neutron attraction between $g_{\frac{7}{2}}$ and $h_{\frac{11}{2}}$ orbitals AND between $g_{\frac{9}{2}}$ and $h_{\frac{11}{2}}$ orbitals
- tensor force should be balanced by central and/or spin-orbit
- no visible tensor effect
- add $h_{\frac{9}{2}}$ for spin-tensor decomposition

Core excitations in Tin isotopes

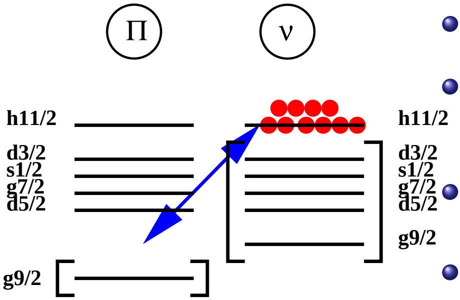

- [132] strongly bound
- low BE2 rates in Tin isotopes towards N=82
- strong proton-neutron attraction between $g_{\frac{7}{2}}$ and $h_{\frac{11}{2}}$ orbitals AND between $g_{\frac{9}{2}}$ and $h_{\frac{11}{2}}$ orbitals
- tensor force should be balanced by central and/or spin-orbit
- no visible tensor effect
- add $h_{\frac{9}{2}}$ for spin-tensor decomposition

Core excitations in Tin isotopes

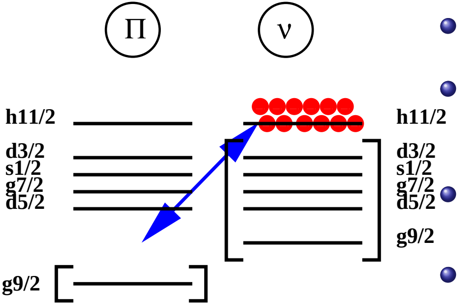

- 132 strongly bound
- low BE2 rates in Tin isotopes towards N=82
- strong proton-neutron attraction between $g_{\frac{7}{2}}$ and $h_{\frac{11}{2}}$ orbitals AND between $g_{\frac{9}{2}}$ and $h_{\frac{11}{2}}$ orbitals
- tensor force should be balanced by central and/or spin-orbit
- no visible tensor effect
- add $h_{\frac{9}{2}}$ for spin-tensor decomposition

powered by LaTeX

Spherical Shell Model and Deformation

- nuclear shell model often considered to be applied only when nuclear manifestations are dominated by single particle degrees of freedom
- BUT work of Elliot: deformation in light nuclei explained by algebraic SU3 model
- Limitations of SU3 model:
  - as the spin orbit term becomes rapidly important its applicability stops at the sd shell
  - but can be recovered approximately as in the pseudo-SU3 or quasi-SU3 schemes.

See:

- A. P. Zuker, J. Retamosa, A. Poves, and E. Caurier
  Phys. Rev. bf C52 (1995) R1741

Deformation in light Xenon isotopes

- In A=100 region, spin-orbit is at play : strong Z=50 shell closure and the $g_{\frac{9}{2}}$ orbital deeply bound with respect to the remaining *gds* orbitals

- the natural valence space beyond ^{100}Sn is made of $g_{\frac{7}{2}}$, $d_{\frac{5}{2}}$, $d_{\frac{3}{2}}$, $s_{\frac{1}{2}}$, and $h_{\frac{11}{2}}$ orbitals

- but at N=Z, $h_{\frac{11}{2}}$ is higher and the other orbitals close to each other

- ➡ one recovers a pseudo-fp space where SU3 symmetry scheme available

powered by LaTeX

Deformation in light Xenon isotopes

- In A=100 region, spin-orbit is at play : strong Z=50 shell closure and the $g_{\frac{9}{2}}$ orbital deeply bound with respect to the remaining *gds* orbitals
- the natural valence space beyond ^{100}Sn is made of $g_{\frac{7}{2}}$, $d_{\frac{5}{2}}$, $d_{\frac{3}{2}}$, $s_{\frac{1}{2}}$, and $h_{\frac{11}{2}}$ orbitals
- but at N=Z, $h_{\frac{11}{2}}$ is higher and the other orbitals close to each other
- → one recovers a pseudo-fp space where SU3 symmetry scheme available

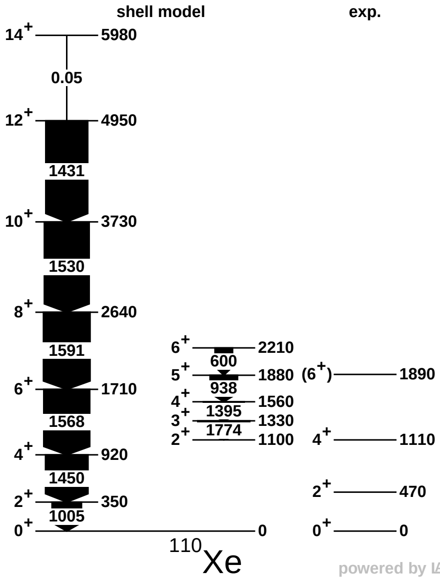

A case of extreme triaxiality: ^{110}Xe

J	E*	E_γ	BE2	Q_{sp}	Q_0 (BE2)	Q_0 (Q_{sp})	β
2^+	0.35	0.35	1005	-62	225	217	0.16
4^+	0.92	0.57	1450	-78	226	215	0.16
6^+	1.71	0.79	1568	-83	224	208	0.16
8^+	2.64	0.94	1591	-87	220	207	0.16
10^+	3.73	1.09	1530	-86	213	198	0.15
12^+	4.95	1.22	1431	-85	204	191	0.15
14^+	5.98	0.99	0.05	-126	1	279	
16^+	6.63	0.69	111	-125	56	273	
18^+	7.51	0.88	1184	-130	183	282	
20^+	8.51	1.00	1043	-134	172	288	
2^+_2	1.10			+61			
3^+	1.33	0.23	1774	-1.3			
4^+_2	1.56	0.23	1395	-38	219	261	0.18
5^+	1.88	0.32	938	-54	217	234	0.17
6^+_2	2.21	0.33	600	-74	209	259	0.17

one could extract the γ from:

$$\frac{BE2(2^+_\gamma \to 2^+_1)}{BE2(2^+_\gamma \to 0^+_1)} \qquad \gamma = 20^o$$

Notice Q(2^+_γ) = - Q(2^+_{Yrast}) and Q(3^+) $\sim$ 0 as results from $3K^2 - J(J+1)$ for K=2 and J=3

Comments about h$_{\frac{11}{2}}$ influence

- reduced M. I. : E(2^+) = 0.19
- slight increase of coll. : BE2(2^+) =1110
- no backbending
- reduced triaxiality $\gamma = 12^o$
- better J(J+1)
- magnetic moments consistent with rot. model up to J=20

Summary

- Continuous Progress in computationnal “standard” diagonalization, and understanding of monopole corrections to 2N forces to provide good spectroscopy
- Monopole drift develops in different regions
- But the physics emerging is quite different:
  - deformation at Z=14, N=28 for ^{42}Si,
  - shell weakening at Z=28, N=50 for ^{78}Ni and
  - strong shell closure at Z=50, N=82 for ^{132}Sn
- Spin-Tensor analysis of the effective interaction in sd-pf show mainly central and tensor components effects
- Spin-Tensor analysis for ^{78}Ni and ^{132}Sn regions under progress to detail relative contributions

Summary

Thanks to:
E. Caurier,
M. Hjorth-Jensen
A. Poves,
K. Sieja,
O. Sorlin
A. Zuker